JOINT TRANSPORTATION
RESEARCH PROGRAM
INDIANA DEPARTMENT OF TRANSPORTATION
AND PURDUE UNIVERSITY

Developing AI-Assisted In-Situ NDT Method for Air-Void Distribution Testing in Fresh and Hardened Concrete

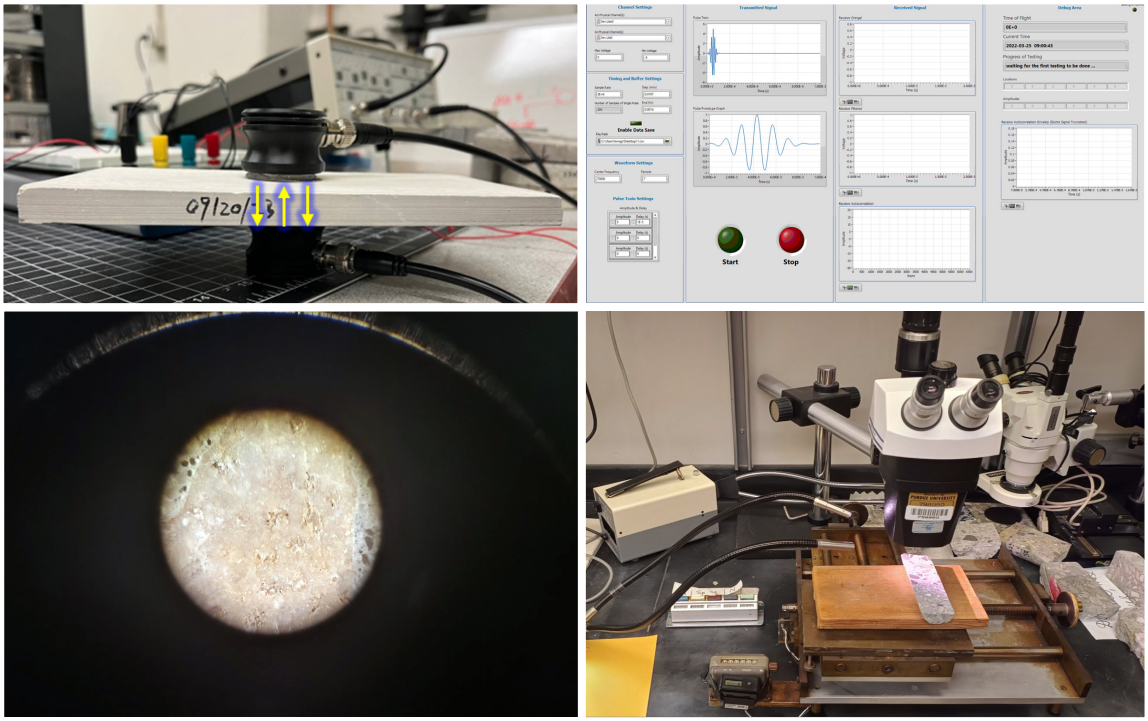

Zhihao Kong, Aritro Roy Mitra, Luna Lu

SPR-4620 • Report Number: FHWA/IN/JTRP-2024/12 • DOI: 10.5703/1288284317745

RECOMMENDED CITATION

Kong, Z., Mitra, A. R., & Lu, L. (2024). *Developing AI-assisted in-situ NDT method for air-void distribution testing in fresh and hardened concrete* (Joint Transportation Research Program Publication No. FHWA/IN/JTRP-2024/12). West Lafayette, IN: Purdue University. https://doi.org/10.5703/1288284317745

AUTHORS

Zhihao Kong
Graduate Research Assistant
Lyles School of Civil Engineering
Purdue University

Aritro Roy Mitra
Graduate Research Assistant
Lyles School of Civil Engineering
Purdue University

Luna Lu, PhD
Reilly Professor of Civil Engineering
Lyles School of Civil Engineering
Purdue University
(765) 494-5842
luna@purdue.edu
Corresponding Author

JOINT TRANSPORTATION RESEARCH PROGRAM

The Joint Transportation Research Program serves as a vehicle for INDOT collaboration with higher education institutions and industry in Indiana to facilitate innovation that results in continuous improvement in the planning, design, construction, operation, management and economic efficiency of the Indiana transportation infrastructure. https://engineering.purdue.edu/JTRP/index_html

Published reports of the Joint Transportation Research Program are available at http://docs.lib.purdue.edu/jtrp/.

NOTICE

TECHNICAL REPORT DUCUMENTATION PAGE

1. Report No. FHWA/IN/JTRP-2024/07	**2. Government Accession No.**	**3. Recipient's Catalog No.**
4. Title and Subtitle Developing AI-assisted In-situ NDT Method for Air-Void Distribution Testing in Fresh and Hardened Concrete		**5. Report Date:** March 2024 **6. Performing Organization Code**
7. Author(s) Zhihao Kong, Aritro Roy Mitra, and Luna Lu		**8. Performing Organization Report No.** FHWA/IN/JTRP-2024/12
9. Performing Organization Name and Address Joint Transportation Research Program Hall for Discovery and Learning Research (DLR), Suite 204 207 S. Martin Jischke Drive West Lafayette, IN 47907		**10. Work Unit No.** **11. Contract or Grant No.** SPR-4620
12. Sponsoring Agency Name and Address Indiana Department of Transportation (SPR) State Office Building 100 North Senate Avenue Indianapolis, IN 46204		**13. Type of Report and Period Covered** Final Report **14. Sponsoring Agency Code**
15. Supplementary Notes Prepared in cooperation with the Indiana Department of Transportation		

16. Abstract

Understanding the air void content in concrete is crucial since it significantly influences the durability and strength of the material, especially in environments susceptible to freeze-thaw cycles. This report introduces an advanced nondestructive testing (NDT) method for the in-situ detection of air voids in concrete by employing diffusive ultrasound. Focusing on the ultrasound attenuation coefficient, this research established a strong correlation with key air void metrics, including the volumetric ratio and spacing factor, as outlined in ASTM C457. The study also undertook a comparative analysis of ASTM C457 methods B and C, revealing the instrument-dependent variability in measuring air voids. One pivotal discovery was that ultrasound attenuation in concrete is majorly influenced by air voids and aggregates, with a relatively minor contribution from cement. This methodology not only offers a novel approach for accurately assessing air void content but also enables visualization of air void distribution in concrete infrastructures like pavements. The findings of this research offer insights for enhancing concrete quality control and ensuring structural integrity in construction, particularly when the in-place air voids conditions are of interest.

17. Key Words concrete, air voids, NDT, ultrasound, diffusive, scattering	**18. Distribution Statement** No restrictions. This document is available through the National Technical Information Service, Springfield, VA 22161.

19. Security Classify. (of this report) Unclassified	**20. Security Classify.** Unclassified	**21. No. of Pages** 20	**22. Price**

Form DOT F 1700.7 (8-72) Reproduction of completed page authorized

EXECUTIVE SUMMARY

Introduction

This technical report outlines the development of a cutting-edge in-situ testing method for assessing air void distribution in concrete, which is a vital factor for ensuring the material's quality and durability. This is particularly relevant for Indiana, a state that experiences harsh winter conditions and multiple freeze-thaw cycles. The proposed testing method aimed to accurately evaluate air void distribution in hardened concrete. Our focus was on the volumetric ratio and spatial distribution of these voids, complemented by the regression model and imaging program.

Existing standard testing methods for fresh concrete, such as ASTM C231 and the Super Air Meter (SAM), exhibited significant variability (around 20%). This variability often leads to issues like reduced strength, shrinkage, freeze-thaw damage, and other durability problems, which are largely due to an incomplete understanding of the spatial distribution of air voids. Our proposed in-situ air void detection technology was designed to identify these issues, thus allowing for intelligent maintenance of concrete structures. Furthermore, recognizing that the phase-changing nature of fresh concrete leads to a variable and uncertain air void system, our project prioritizes the assessment of air voids in hardened concrete. Our air void estimation method was founded on diffusive ultrasound theory, which represents concrete as a three-component system. This method primarily employs ultrasound attenuation as a quantitative metric, facilitating a direct regression to air void characteristics. Empirical data revealed a strong correlation between air void content and ultrasound attenuation, indicating the method's accuracy and reliability in concrete analysis.

Findings

In this research, we investigated multiple methods commonly used in biomedical engineering and geotechnical fields for estimating the air void system in concrete. The diffusive ultrasound method stood out for its practical applicability and robust physical foundation.

Our approach models concrete as a three-component system—cement paste, aggregates, and air voids—each contributing distinctly to the ultrasound signal's total attenuation. This model facilitates precise analysis of how ultrasound waves are attenuated differently by each concrete component. To isolate the impact of air voids on ultrasound attenuation, we systematically varied material components in a controlled experimental setup, excluding air voids, thereby establishing a direct correlation between air void content and ultrasound attenuation.

Additionally, we quantified ultrasound attenuation in pure cement paste samples and benchmarked these measurements against those from concrete samples. This comparison elucidated the relative contribution of cement paste to overall absorption attenuation. The key findings and outcomes of this project, pivotal in advancing air void system estimation, are detailed in the subsequent sections.

1. *Theoretical model of ultrasound attenuation caused by concrete material.*

   We investigated several models that describe mechanical wave properties in porous elastic materials, such as petroleum basins, and solid materials with cavities, like bone trabeculae. Biot's theory emerged as a significant reference, delineating the propagation of both fast and slow waves through such materials. The theory's differentiation between these wave types provides a nuanced understanding of how sound waves interact with complex structures.

   We also examined the dual-frequency method, which involves the interplay of a pump wave and a probe wave. This method was particularly useful in distinguishing between different types of wave interactions within a medium and offering insights into the material's structural composition and characteristics.

   Ultimately, our decision to utilize diffusive ultrasound for quantifying air void distribution in concrete was driven by its effectiveness in capturing the intricate details of wave propagation through heterogeneous materials. This approach leveraged the scattering and absorption of ultrasound waves within the concrete to accurately map the distribution and size of air voids. By focusing on the attenuation characteristics of ultrasound waves as they pass through concrete, the diffusive ultrasound model provides a reliable and precise method for assessing the internal structure of concrete, particularly air void content and distribution.

2. *Custom pulser-receiver set-up and precautions.*

   Our study led to the development of an advanced pulser-receiver system that was capable of finely tuning operation frequency and voltage and was supplemented by controlled timing and the capacity for repetitive measurements. Empirical data suggests that averaging over at least 20 repeated tests substantially improves the signal-to-noise ratio (SNR), thus enhancing the precision in calculating the attenuation coefficient. This testing apparatus also supports the use of varied wavelengths. However, caution is necessary when selecting the operational wavelength to ensure clear discrimination between the first and second reflected waves and avoiding aliasing effects. It is important to acknowledge that our testing protocol involved surface polishing of the sample and the application of coupling gel, a significant limitation for the practical application of this technology and similar acoustic-based non-destructive evaluation (NDE) methods. To overcome this challenge, our research is now focused on developing dry point contact transducers, which could eliminate the need for these preparatory steps and streamline the overall testing process.

3. *High correlation of ultrasound attenuation coefficient to air void parameters.*

   To establish the relationship between the ultrasound attenuation coefficient and air void parameters, we conducted tests in accordance with ASTM C457, *Standard Test Method for Microscopical Determination of Parameters of the Air-Void System in Hardened Concrete* (ASTM, 2010). We implemented both Procedure B (point-counting microscope method) and Procedure C (chord length scanning microscope method). Target metrics included the volumetric ratio and spacing factor of air voids. We employed polynomial regression to assess the correlation between the ultrasound attenuation coefficient and these target metrics. The results yielded a high R2 value of 0.924 for the volumetric ratio and 0.982 for the spacing factor. These findings reveal a direct relationship: the volumetric ratio of air voids positively correlates with the ultrasound attenuation coefficient, while the spacing factor shows a negative correlation. In simpler terms, a higher concentration of air voids leads to increased acoustic attenuation, whereas a sparser distribution of air voids results in lower acoustic attenuation. These trends are consistent with theoretical expectations, thus validating the robustness of our methodology.

CONTENTS

LIST OF TABLES

LIST OF FIGURES

1. INTRODUCTION

1.1 Research Background

This research project, focusing on the development of an AI-assisted in-situ non-destructive testing (NDT) method for air-void distribution in concrete, is positioned at the intersection of cutting-edge technology and practical engineering needs. It addresses the critical challenge of accurately assessing air void distribution in hardened concrete, crucial for ensuring concrete quality and durability, especially in harsh environments like Indiana's multiple freeze-thaw cycles (shown in Figure 1.1) and winter conditions. Leveraging the expertise in ultrasound sensing, materials science, and AI-driven signal processing, the project aims to introduce a novel, nondestructive method for air void testing by investigating the acoustic scattering nature of poroelastic materials, such as concrete, with AI-assisted signal processing techniques. This approach will enable the accurate determination of air-voids size and spatial distribution in lieu of tedious lab procedure shown in Figure 1.2, and assist in predicting the locations of pavement failure due to environmental and physical stressors. The research is built on a foundation of established scientific principles and utilizes advanced methodologies like diffusive ultrasound and customized pulser-receiver setups for empirical investigations. This comprehensive approach combines theoretical modeling, numerical simulation, and experimental validation to develop a robust, field-applicable NDT method for air void analysis in concrete.

1.2 Objectives

In this research project, we are dedicated to advancing the understanding and assessment of air void systems in concrete. The following objectives are instrumental in achieving this goal, encompassing both theoretical development and practical application.

1. *Air Void Distribution Analysis:* Focusing on developing a sophisticated method for analyzing air void size distribution in hardened concrete, utilizing state-of-the-art ultrasonic technology and AI-driven data interpretation.
2. *Innovative Theoretical and Practical Development:* Aimed at bridging theoretical models with real-world applications in concrete assessment, leading to novel solutions and methodologies in material science.
3. *Imaging for Engineering Application*: Developing an AI-based program to effectively visualize and analyze air void distribution, providing crucial insights for engineering applications and concrete quality assessment.

1.3 Organization of the Report

This report consists of five chapters. This first chapter introduces the background and objective of this research. The second chapter reviews existing testing methods for air voids in concrete. The third chapter reports our experiment work for the validation of the proposed air void testing method. The fourth chapter presents the testing results. The final chapter summarizes the current works and concludes this report.

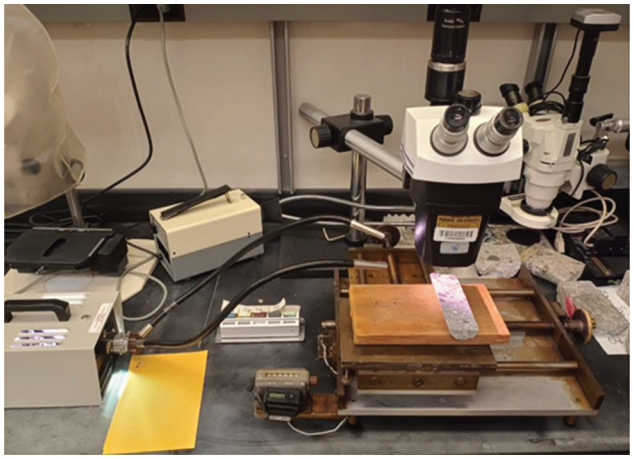

Figure 1.2 ASTM C457 testing instruments.

(a) 0 cycles of freeze-thaw (b) 200 cycles of freeze-thaw (c) 400 cycles of freeze-thaw

Figure 1.1 Freeze-thaw effect on concrete sample (Shang & Yi, 2013).

2. LITERATURE REVIEW

2.1 Air Void System of Concrete

2.1.1 Classification of Air Voids

In hardened cement paste, voids are categorized into four types: gel pores, capillary pores, entrained air, and entrapped air. Gel pores are the smallest, ranging from 0.5 to 2.5 nm, and do not significantly affect the strength and permeability of cementitious materials, but they do impact drying shrinkage and creep. Capillary pores, slightly larger, can be up to 1 μm in size and are not filled by hydration product solids. The dimensional range of air voids in hydrated cement is shown in Figure 2.1. Their size is largely determined by the initial spacing between cement particles and hydration levels. Capillary pores larger than 50 nm, termed macropores, affect strength and permeability, while smaller ones, known as micropores, function similarly to gel pores.

Entrained air voids, ranging from 50 to 1,000 μm, are introduced via air entrainments to enhance frost resistance. In contrast, entrapped air voids are larger, irregularly shaped, and less in number compared to entrained air. Both entrained and entrapped air voids influence concrete's strength, particularly the larger pores.

2.2 Existing Air Void Characterization Methods

2.2.1 ASTM C 457 for the Air-Void System in Hardened Concrete

ASTM C457 is a well-established method for analyzing air-void systems in hardened concrete, crucial for assessing concrete's freeze-thaw durability. This method involves microscopical examination to determine air void parameters like size, spacing, and distribution. It's recognized for its precision in evaluating the air-void system, crucial for concrete's resistance to environmental damage. However, ASTM C457 is a time-consuming process (as shown in Figure 2.2 and Figure 2.3) requiring polished concrete samples and microscopic or automated image analysis, limiting its use to post-construction diagnostics rather than real-time adjustments during construction. The test results from ASTM C457 can exhibit a variability of more than 25% (Saucier et al., 1996; Simon, 2005), reflecting the method's sensitivity to sample preparation and analysis techniques. Despite these challenges, ASTM C457 remains a widely accepted and critical method for air-void system analysis in hardened concrete.

2.2.2 ASTM C 231 for the Air-Void System in Fresh Concrete

ASTM C231 is a critical standard for assessing air content in freshly mixed concrete, using the pressure method, as shown in Figure 2.4. This method, grounded in Boyle's Law, involves pressurizing a concrete sample within a calibrated chamber. The resultant volume change quantifies the air content, a key indicator of concrete's durability, especially in freeze-thaw conditions. ASTM C231 is indispensable in concrete mix design and quality control, ensuring the structural integrity and longevity of concrete structures in varying environmental conditions.

2.3 Air Voids Quantification Theories

2.3.1 Ultrasound Attenuation in Solid Material with Inhomogeneous Spherical Inclusions

The ultrasonic scattering theory used to calculate energy loss caused by scattered objects was established

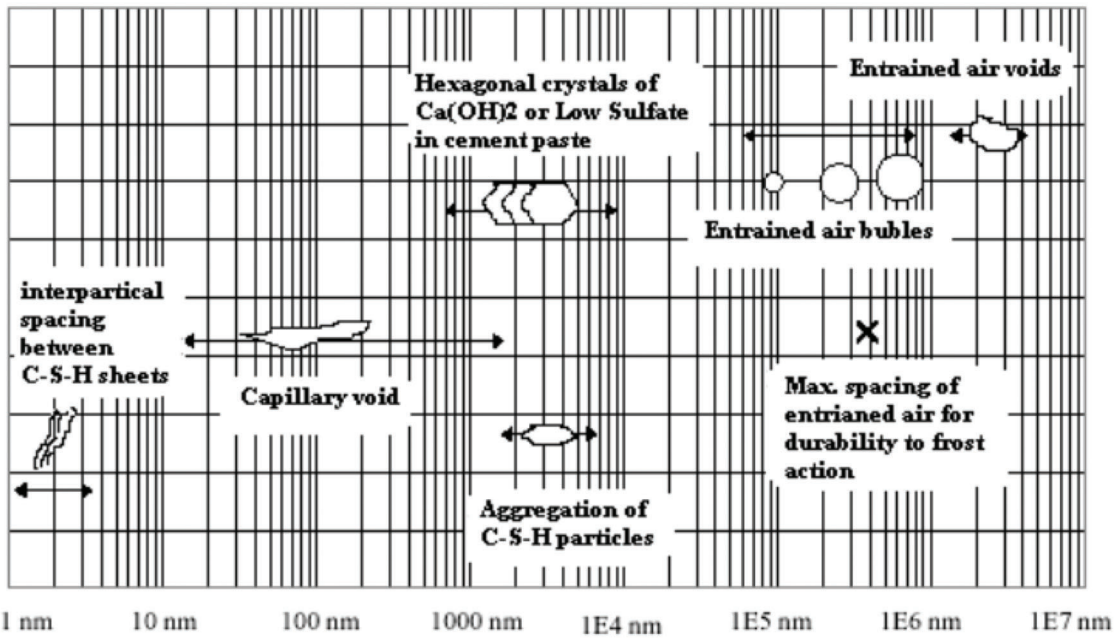

Figure 2.1 Dimensional ranges of voids in hydrated cement paste (Mehta & Monteiro, 2014).

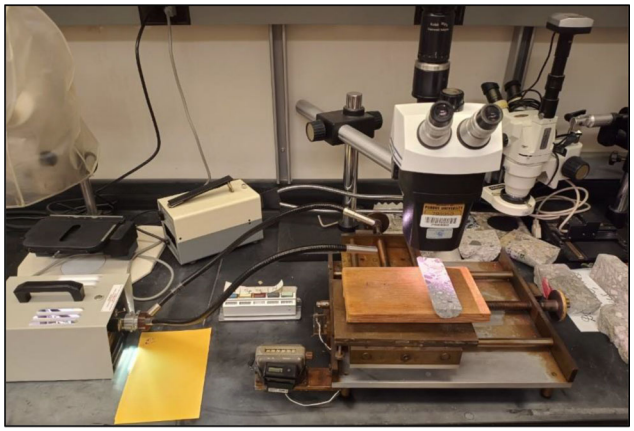

Figure 2.2 ASTM C457 Method B instrument.

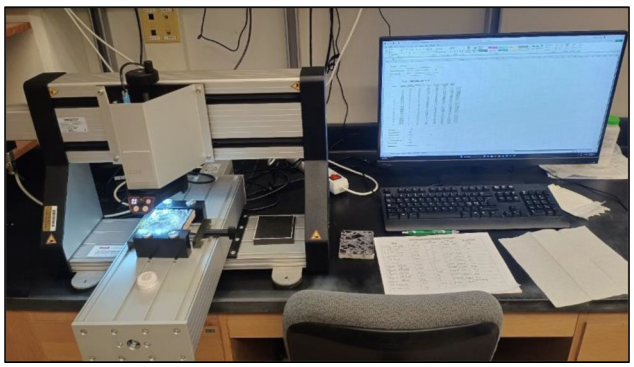

Figure 2.3 ASTM C457 Method C instrument (RapidAir).

by Ying and Truell (1956). The theory is based on the equation of motion in homogeneous solid materials when the wave function is only related to space variables. It provides a theoretical model to calculate the influence on the wave attenuation for obstacles like air voids and aggregates. The shape of air voids in the hardened concrete has minimal influences on its strength properties. In this research, both small air voids and large air voids are considered to be a distribution of spherical voids with different sizes. The theoretical attenuation can be expressed by combining the effects of the viscous matrix and scattering due to aggregates and air voids.

$$\alpha(f)=(1-\phi)\alpha_a(f)+\frac{1}{2}\sum_{i=1}^{m1}n_{i,1}\gamma_{i,1}^{sca}(f)+\frac{1}{2}\sum_{i=1}^{m2}n_{i,2}\gamma_{i,2}^{sca}(f)$$

where $\alpha(f)$ is the total attenuation coefficient in Nepper per meter (Np/m) of the ultrasonic wave absorbed by the hardened concrete; ϕ is the combined volume fraction of the air voids and aggregate (%); $\alpha_a(f)$ is the attenuation coefficient of the viscoelastic cement paste (Nepper/m); $n_{i,1}$ and $n_{i,2}$ are the numbers of a certain size aggregate and air void per volume, respectively; $\gamma_{i,1}^{sca}(f)$ and $\gamma_{i,2}^{sca}(f)$ represent the

Figure 2.4 ASTM C231 instrument.

corresponding scattering cross sections of the aggregate and air voids, respectively.

The scattering cross section is defined as the equivalent area of a scatterer and is larger than the physical area of the scatterer—it is the ratio of the scattered power divided by the intensity of the incident wave. This calculation is a classical problem of wave scattering (associated with the scalar Helmholtz equation) and has been addressed by several researchers. The calculation for aggregates and air voids were given below (Ying & Truell, 1956).

The calculation of the scattering cross sections $\gamma_{i,1}^{sca}(f)$ follows the theoretical derivation of Ying and Truell (1956).

$$\gamma_{elastic\ sphere}=\frac{4\pi}{9}g_e k_1^4 a^6$$

$$g_e=\left(\frac{3\frac{\kappa_1^2}{k_1^2}}{\left(3\frac{\kappa_2^2}{k_2^2}-4\right)\frac{\mu_2}{\mu_1}+4}-1\right)^2+\frac{1}{3}\left(1+2\left(\frac{\kappa_1}{k_1}\right)^3\right)\cdot\left(\frac{\kappa_2}{\kappa_1}\frac{\mu_2}{\mu_1}-1\right)^2$$

$$+40\left(2+3\left(\frac{\kappa_1}{k_1}\right)^5\right)\cdot\left(\frac{\frac{\mu_2}{\mu_1}-1}{2\left(3\left(\frac{\kappa_1}{k_1}\right)^2+2\right)\frac{\mu_2}{\mu_1}+9\left(\frac{\kappa_1}{k_1}\right)^2-4}\right)^2$$

where κ_1 and k_1 are the wave number of S wave and P wave of the cement paste, respectively; κ_2 and k_2 are the wave number of S wave and P wave of the aggregates, respectively; μ_1 and μ_2 are the Poisson's ratio of the cement paste and aggregate, respectively.

The calculation of the scattering cross sections $\gamma_{i,2}^{sca}(f)$ follows the theoretical derivation of Ying and Truell (1956).

$$\gamma_{sphere\ cavity} = \frac{4\pi}{9} g_c k_1^4 a^6$$

$$g_c = \frac{4}{3} + 40\frac{2+3\left(\frac{\kappa_1}{k_1}\right)^5}{\left(3\left(\frac{\kappa_1}{k_1}\right)^2\right)^2} - \frac{3}{2}\left(\frac{\kappa_1}{k_1}\right)^2 + \frac{2}{3}\left(\frac{\kappa_1}{k_1}\right)^3 + \frac{9}{16}\left(\frac{\kappa_1}{k_1}\right)^4$$

2.3.2 Ultrasound Attenuation in Solid Material with Homogeneous Spherical Inclusions

In the work of Punurai et al. (2006, 2007) a simplified scenario is studied where all air voids in cement paste are of identical size and there are no aggregates in the mixture, see Figure 2.5. Then the air voids system can be defined simply using two metrics, i.e., the volumetric ratio ϕ, and the diameter of air voids a.

The problem to solve the combination of (ϕ, a) from the experimentally measured attenuation curve

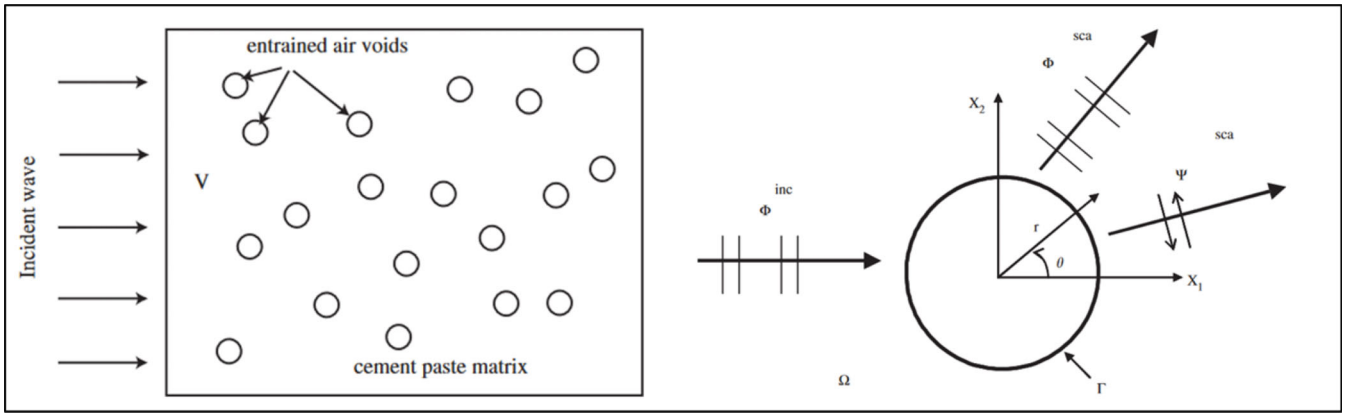

Figure 2.5 Simplified acoustic wave scattering model (Punurai et al., 2006).

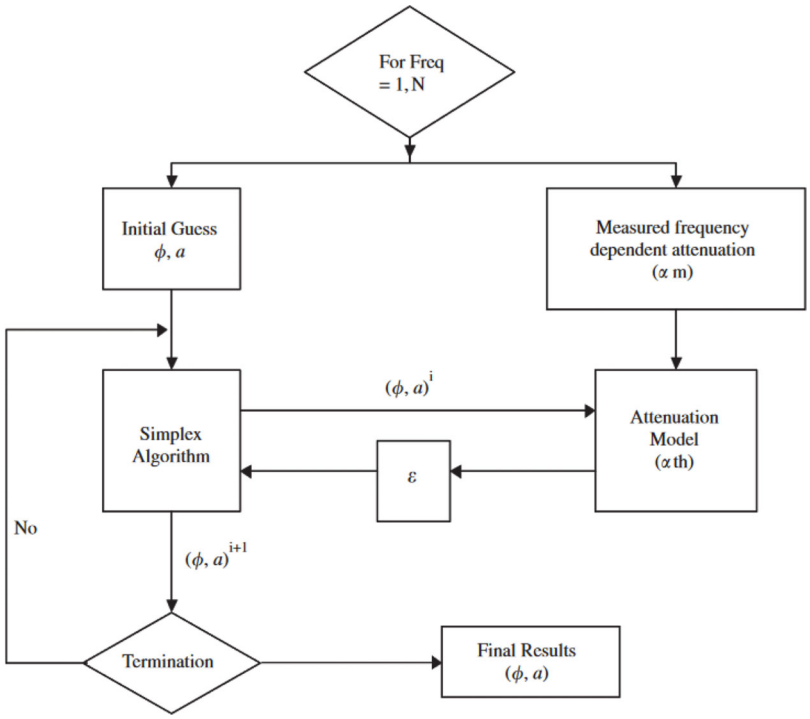

Figure 2.6 Optimization algorithm for (ϕ, a) determination (Punurai et al., 2006)

$\alpha(f)$ is an inverse problem that can be addressed using optimization algorithms, such as Simplex method.

The objective function of the optimization task is the difference between the calculated theoretical attenuation curve and the actual experimental attenuation curve. A pair of (ϕ_0, a_0) is initiated at the beginning of the algorithm, then the (ϕ_i, a_i) is updated iteratively with the aim of making the loss function reach a convergence.

The authors reported promising prediction results compared to ASTM C457 results. The ultrasound predicted air content is consistently lower than that of ASTM results. The authors believe the ultrasound method is more representative of the actual entrained air content in the specimens because the method is more sensitive to smaller air voids.

To apply the aforementioned ultrasound techniques to this research, we start with a more simplified scenario where the distribution of aggregates is known and controlled the same across the experiments, the total volumetric ratio ϕ is then correlated with the attenuation curve $\alpha(f)$.

3. EXPERIMENTAL STUDY

This chapter reports the experimental work of studying the correlation of ultrasound metrics and air void system parameters. We use the results of ASTM C 457 as the reference target.

3.1 Mixture Design

Mixture designs with constant cement content and varying Air Entrainment Agent (AEA) dosage were used for this research. The 0.535 water-to-cement ratio (w/c) mixtures were chosen, following the existing study in literature (Guo, 2016), and they bracket the range of typical w/c with decent workability. To investigate the effect of air content, a series of AEA dosages was investigated. A higher dosage of AEA, 3.0 ml/cem.kg, was used in the mixtures, which will be targeted for 7% total air content. A medium dosage of 1.0 ml/cem.kg was used which will be targeted for 5% total air content. A dosage of zero AEA was used as the reference group, with which the air content is expected to be around 3%. Different dosages were used to simulate the different ranges of typical AEA dosages used in the field. All of these dosages were within the manufacturer (Sika) recommended limits. Ingredients other than the AEA dosage were controlled the same so the contribution of the single variable can be studied. Table 3.1 shows the mixture design proportions.

3.2 Concrete Mixture Procedure

In this research, aggregates were initially accessed from outdoor storage and heated in a drying oven at 215°F for a minimum of 12 hours prior to mixing. They were then placed in a mixer, rotated to ensure homogeneity, and a representative sample was extracted for moisture content adjustment, as shown in Figure 3.1. During mixing, all aggregates were combined with about two-thirds of the mixing water in the mixer, agitated for three minutes to promote a saturated surface dry (SSD) state and uniform distribution. Subsequently, Air-Entraining Agent (AEA), if used, was blended into the remaining water for one minute, then introduced into the mixer. Following the AEA's addition, the concrete mixture was further mixed for three minutes, ensuring thorough incorporation of the admixture.

The casting of fresh concrete was conducted in 4 by 8-inch cylindrical molds, adhering to ASTM C31 guidelines. Each cylinder was filled in two layers, with each layer compacted 25 times using a rod for uniform consolidation. Alongside the concrete cylinders, companion cement paste slabs, measuring 4 by 8 by 1 inch and using identical mixture proportions, were prepared for each mixture design. These slabs were specifically crafted to measure the "background" ultrasound attenuation in concrete, attributable to the absorption effect of the cement paste, providing a control for the air void analysis.

The air void system of each concrete mixture was analyzed at 1 day, 3 days, and 7 days. For each age, two cylindrical concrete samples were prepared. Additionally, a single cement paste slab was used for each mixture design across all ages, as it did not require saw cutting. Consequently, a total of six cylinders and one cement slab were cast for each mixture design. Both the concrete cylinder samples and the cement slab samples underwent a curing process in a controlled environment, maintained at a steady temperature of 73°F.

3.3 Sampling of Hardened Concrete

At each designated age (1 day, 3 days, and 7 days), two concrete cylinder samples were sectioned to form slabs. One slab per sample was allocated for ASTM C457 testing, and the other for ultrasound testing. The hardened air void samples were sliced into 1-inch-thick sections using a self-propelled concrete saw equipped with an 18-inch diameter continuous rim blade. After the cutting, the concrete samples were thoroughly cleaned with water and subsequently dried in an oven at 140°F (60°C) for 1 hour. A concrete lapper was utilized to prepare the samples according to ASTM C 457 specifications, ensuring they were suitably conditioned for accurate testing.

Once lapping was completed, each sample was examined under a stereomicroscope to verify uniform lapping of aggregates and paste to the same elevation, ensuring a high-quality surface finish. For ASTM C457 analysis, the concrete slab's surface was marked uniformly with black permanent marker and allowed to dry for 3 hours. A thin layer of barium sulfate, a white powder, was then applied twice to the colored surface using a rubber stopper to embed the powder into the voids, as prescribed in ASTM C457.

TABLE 3.1
Mixture Design

Mixture	Cement (kg/m^3)	Coarse Aggregates (kg/m^3)	Fine Aggregates (kg/m^3)	Water (kg/m^3)	w/c	AEA Dosage (ml/kg of cement)	Sika Air 260 AEA (ml/m^3)	Target Air Percentage (%)
1	334.6	1,110.7	740.4	179.01	0.535	0	0	3
2						1	334.6	5
3						3	1,003.8	7

Figure 3.1 Aggregates preparation.

This process resulted in a contrast between the black surface and the white-stained voids. The focus being on paste voids, aggregate voids were individually marked with a fine ink pen under the microscope. A final inspection confirmed the distinction between white voids in the paste and the uniformly black other areas. Polished and finished sample images are presented in Figure 3.2. This technique, detailed in literature (Jakobsen et al., 2006; Jana, 2007; Song et al., 2017) ensures the precise void analysis.

3.4 Air Void Testing of Hardened Concrete Following ASTM C457

After selectively marking the voids in the paste, the contrast thus created was utilized to assess the air void parameters in the concrete mixture. The team employed the Rapid Air 457 from Concrete Experts, Inc., a device that conducts automated linear traverse analysis. This is achieved through a CCD camera that captures images of the sample's surface and an automated stage for precise positioning. Image analysis software then differentiates the voids (white) from the rest of the sample (dark), as shown in Figure 3.3. For all samples, a consistent threshold value of 128 was used, a level proven effective given the materials and methods of sample preparation. The paste volume of the hardened concrete was calculated with the procedure mentioned in the ASTM C457 Method B. In the hardened air void analysis within this document, chords smaller than 30 μm were excluded as their detection is challenging in manual ASTM C 457 analyses. Omitting these chords aligns the air void parameters from this study more closely with conventional ASTM C 457 results. This approach of exclusion for improved comparability has been previously adopted in previous studies (Jakobsen et al., 2006; Ley, 2007; Peterson et al., 2009).

3.5 Ultrasound Testing Procedure

Commercial contact transducer pairs (0.5 MHz nominal frequencies, Panametrics Inc.) are used along with a custom pulser–receiver to transmit longitudinal (or transverse) ultrasonic waves into each of these specimens. The electrical signal is first amplified with a maximum of ± 150 V with a power amplifier. The transmitting transducer (T) then converts the electrical signal to a pressure wave. The pressure wave propagates through a specimen and is received by another transducer (R) and converted into the electrical signal. The signal is acquired with a sampling rate of 2 mega samples per second, and with 32-bit resolution with a digital oscilloscope. The signal-to-noise ratio (SNR) is increased by averaging over a number of signals

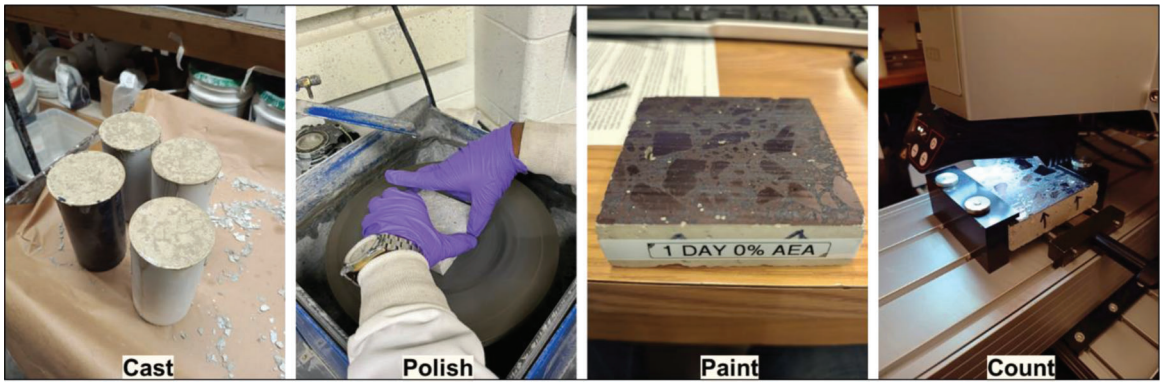

Figure 3.2 Concrete sample preparation for ASTM C 457.

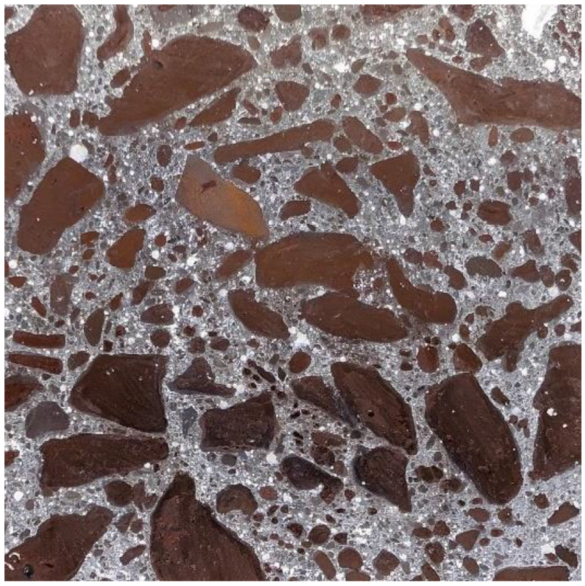

Figure 3.3 Painted concrete sample for image analysis of air voids.

(i.e., 20). The testing set-up and the front panel of the data collection program designed using LabVIEW are shown in Figure 3.4 and Figure 3.5, respectively.

The spectrum of each received signal is calculated using a fast Fourier transform (FFT) procedure. Spectral ratio analysis is used to measure the attenuation coefficient; this technique compares the amplitude and phase spectra of two signals recorded on the same specimen which have traveled along two different paths. The process of spectral ratio analysis is detailed below.

As shown in Figure 3.6, the first signal, $s_1(f)$, propagates through one thickness of the specimen (direct longitudinal or transverse wave), while the second signal, $s_2(f)$, propagates through three thicknesses of the same specimen after reflections on both

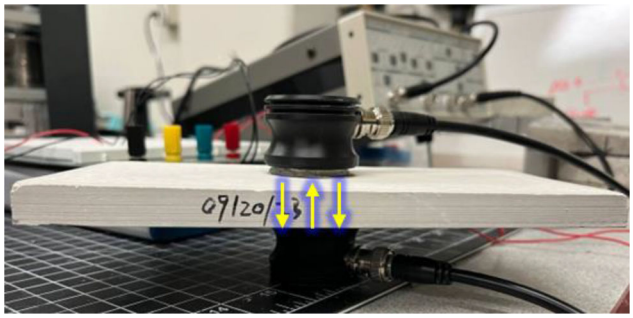

Figure 3.4 Ultrasound testing setup.

specimen sides. With a pair of finite circular transducers, the amplitude spectra of the two signals are:

$$\alpha(f) = \frac{1}{2d} \log \frac{s_1(f)}{s_2(f)}$$

where $\alpha(f)$ is the attenuation coefficient, d is the thickness of the sample, $s_1(f)$ is the frequency spectrum of the first signal, and $s_2(f)$ is the frequency spectrum of the second signal.

Prior to examining ultrasonic attenuation in concrete specimens, the system's accuracy was verified using a polymethylmethacrylate (PMMA) sample. The sample, situated between the "pulser" and "receiver" transducers, utilized a couplant to minimize coupling effects. The first and second transmission waves were captured and transformed into frequency spectra via Fourier transformation for attenuation assessment. The attenuation coefficient curve was computed, and the results are displayed in Figure 3.7. Additionally, transmission speed was deduced from the first transmission signal's arrival time and sample thickness. These results closely align with reference values in (Guo et al., 2017), as illustrated in Figure 3.8, validating the system's precision in attenuation measurement.

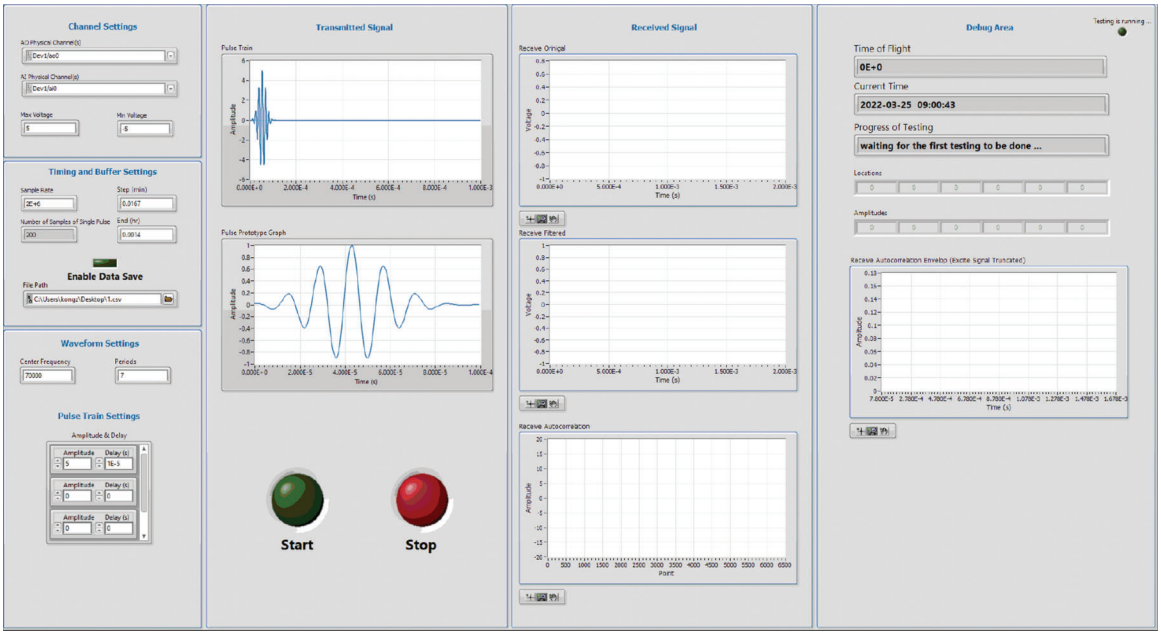

Figure 3.5 Front panel of the control program.

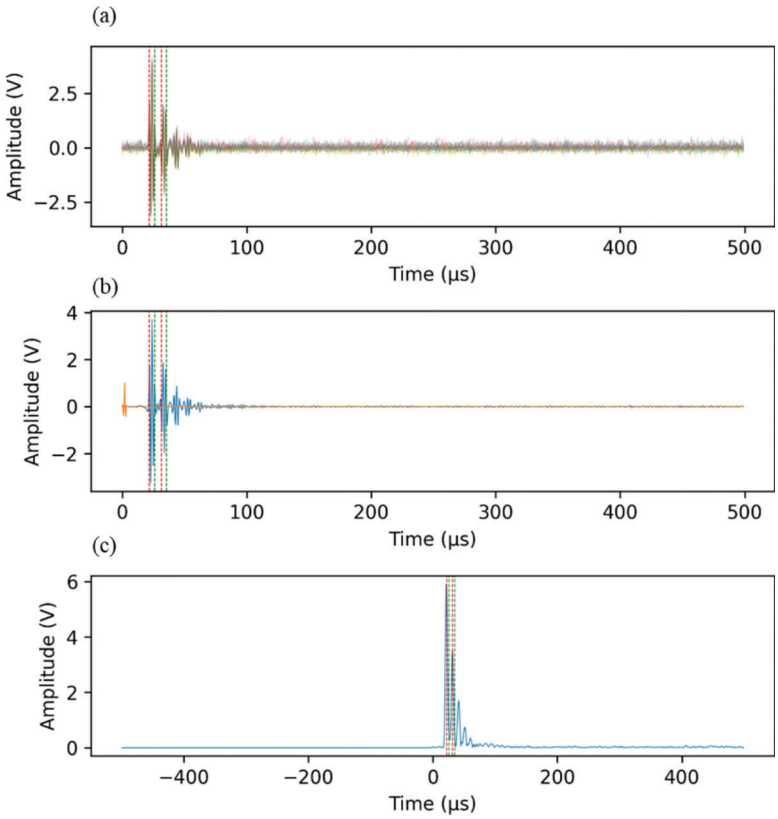

Figure 3.6 (a) Raw time domain signals, (b) averaged time domain signal, and (c) cross-correlation profile of the transmitted wave and received wave.

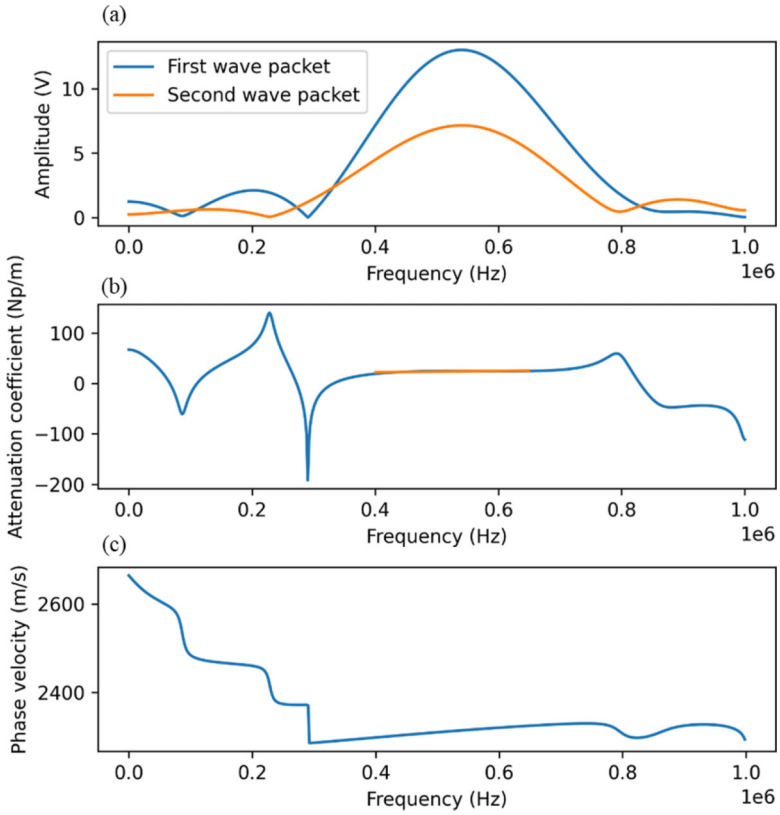

Figure 3.7 (a) Frequency spectrum of the first and second wave packet, (b) attenuation coefficeint curve, and (c) phase velocity.

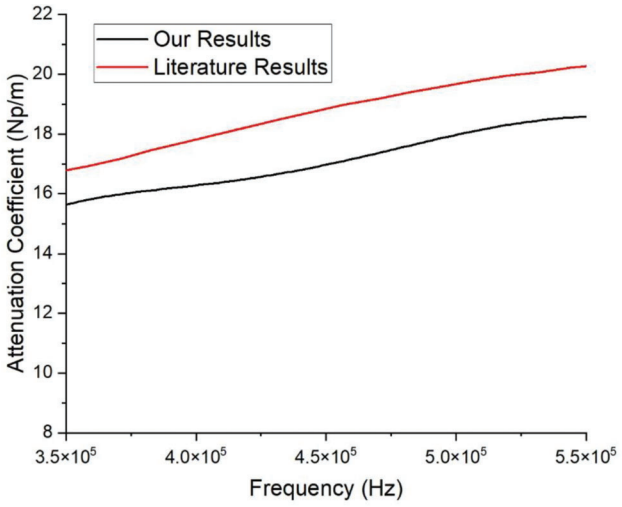

Figure 3.8 Comparison of the attenuation coefficient curve measured by the researchers vs. literature results for PMMA material (Guo et al., 2017).

4. RESULTS

The traditional ASTM C457 results and ultrasound testing results are presented in this section. The difference between Procedure B (manual modified point count) and Procedure C (automated contrast enhanced method) results are also presented in this section.

4.1 ASTM C457 Results

We first present the relationship between the spacing factor and air content of hardened concrete samples in Figure 4.1. The metrics of air voids were measured following ASTM C457 Method C unless otherwise clarified in the following parts of this report. The air content of our samples ranges from 1.83% to 7.15% and the spacing factor ranges from 0.19 mm to 0.31 mm. The spacing factor decreases when the total air content increases, following a power trend $y = 0.3566x^{-0.2927}$ with $R^2 = 0.607$. A similar statistical relation was also reported in literature (Zhang et al., 2020), as shown in Figure 4.2, therefore, our testing procedure and results of the air content and spacing factor are reliable.

Furthermore, we studied the variance of the measurement results caused by different procedures of ASTM C457, including the Method B, Modified Point Count Method, and Method C, Image Processing Method. The results of both methods are presented in Figure 4.3. The air content measured by Method C tends to be higher than that of Method B when the air content is less than 5% and lower than Method B when the air content is higher than 5%. In general, the two methods align good with each other. The discrepancy is mostly less than 0.5%. We also observed the variance of air content results caused by instruments in literature (Jana, 2007).

As shown in Figure 4.4, various image processing methods were compared with the modified point

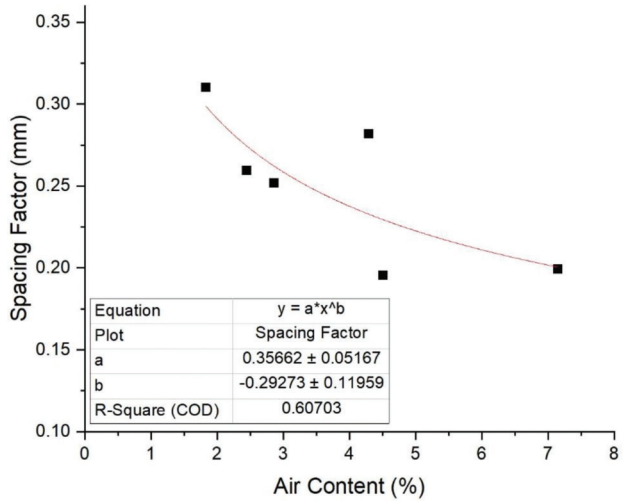

Figure 4.1 Spacing factor vs. air content results.

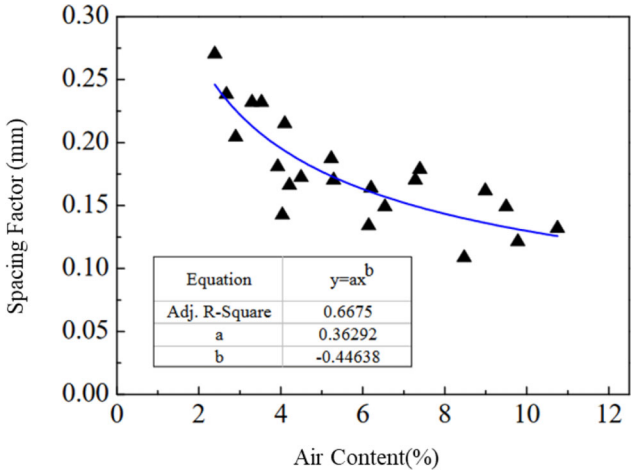

Figure 4.2 Spacing factor vs. air content result from literature (Zhang et al., 2020).

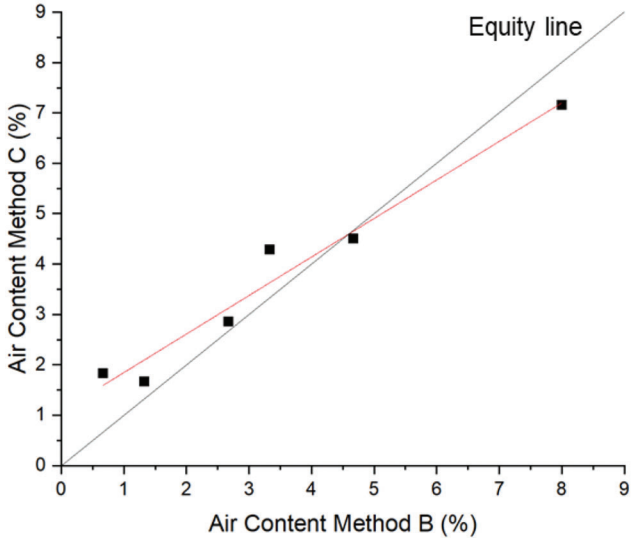

Figure 4.3 Air content results of Method C vs. Method B.

counting method. The air content results by image processing can be either higher or lower than Method B results, so the relative relationship between Method B and Method C is instrument dependent. We choose to use Method C results as the ground truth of air void metrics considering the discrepancy between Method C and B is small and Method C procedure has been widely adopted.

4.2 Ultrasound Results

The ultrasound signals were processed following the procedures in Section 3 and the metrics of ultrasound

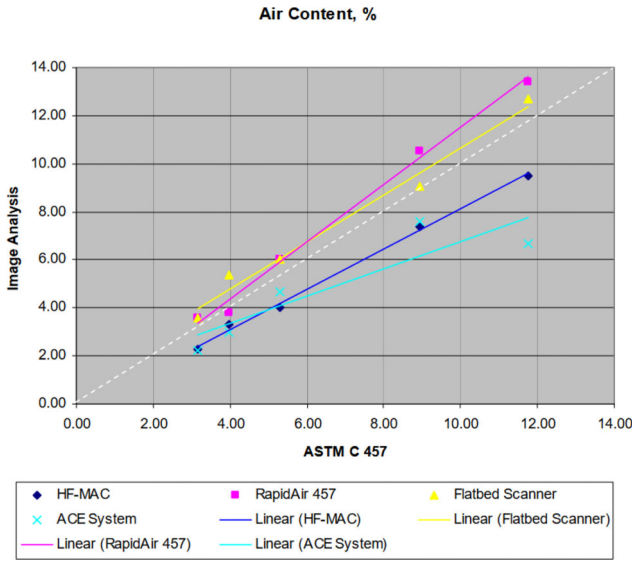

Figure 4.4 Air content results of various image processing methods vs. Method B (Jana, 2007).

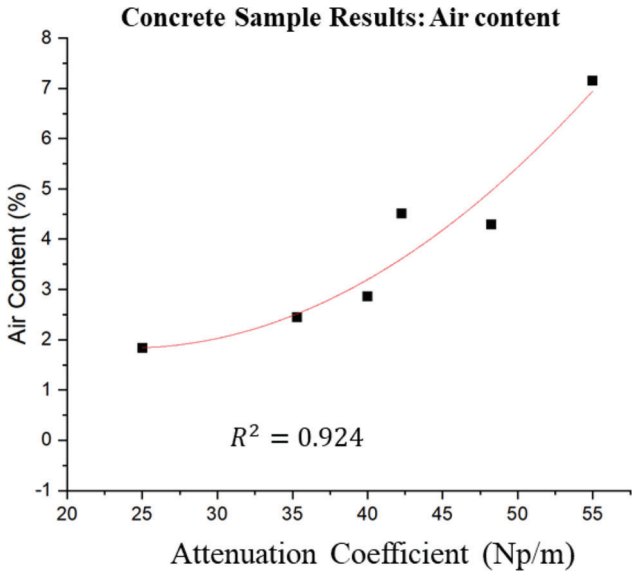

Figure 4.5 Correlation between the air content measured by ASTM C457 Method C and the ultrasound attenuation coefficient.

are correlated with the metrics of air voids of concrete. As shown in Figure 4.5, the volumetric ratio of air content exhibits a strong correlation (R^2 = 0.924) with the power function of attenuation coefficient.

On the other hand, as shown in Figure 4.6, the spacing factor of air voids has a linear correlation (R^2 = 0.982) with the attenuation coefficient of ultrasound if two outlier points are excluded. In addition to analyzing the total attenuation caused by concrete, we measured the attenuation caused by the cement paste to quantify the contribution of the scattering effect versus absorption effect. As shown in Figure 4.7, the attenuation coefficient caused by cement paste is 24.67 Np/m, which is below the lower bound of all concrete samples. Whereas the total attenuation coefficient of concrete ranges from 25 Np/m to 55 Np/m, revealing that the energy scattering by aggregates and air voids holds the primary part of the total attenuation of ultrasound signal.

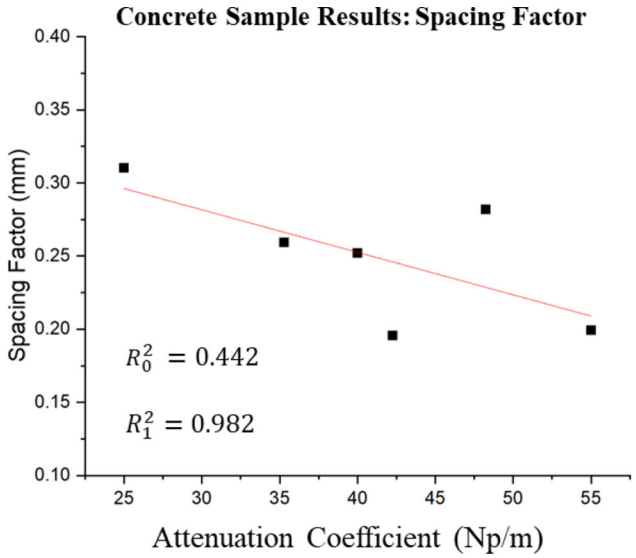

Figure 4.6 Correlation between the air void spacing factor measured by ASTM C457 Method C and the ultrasound attenuation coefficient.

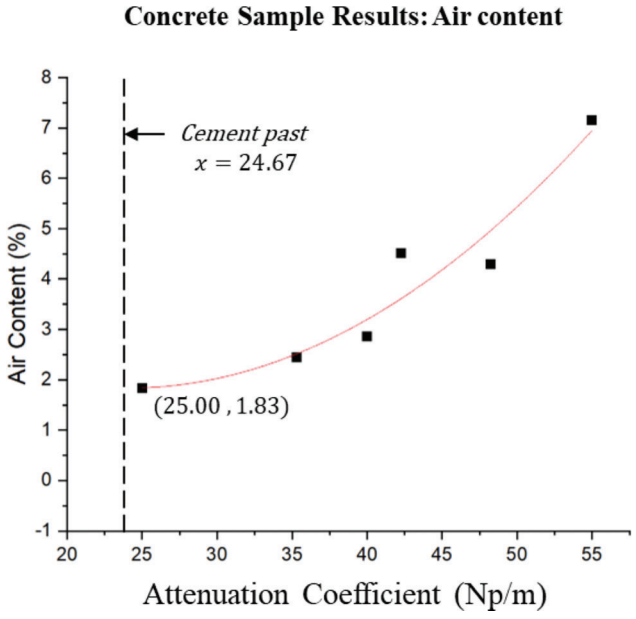

Figure 4.7 Attenuation contributed by the cement paste.

5. CONCLUSIONS

Our study in this project has yielded significant insights into the relationship between ultrasound attenuation coefficients and the air void characteristics of concrete. A notable finding is the effectiveness of the ultrasound attenuation coefficient as a metric to correlate with concrete air void metrics. This was evidenced by its R^2 value of 0.924 with the volumetric air content and an R^2 of 0.982 with the spacing factor, indicating a reliable degree of correlation.

In our exploration of ASTM C457 Methods B and C, we observed that the relationship between ultrasound attenuation and concrete air void characteristics appears to be instrument-dependent, suggesting a lack of determinism in this relationship.

Furthermore, our analysis revealed that the attenuation caused by concrete is predominantly due to air voids and aggregates. The contribution of cement to this attenuation is comparatively minor. This highlights the substantial influence of air voids and aggregates on the ultrasound attenuation properties of concrete, a factor that must be taken into account in both practical applications and future research.

In conclusion, the findings from this project provide valuable contributions to the understanding of ultrasound attenuation in concrete. They emphasize the importance of considering instrument variability in concrete assessment and offer a new perspective on the contributions of different concrete components to ultrasound attenuation. These insights have potential implications for improving non-destructive testing methods and enhancing the overall understanding of concrete properties.

REFERENCES

ASTM. (2010). *ASTM C457-09: Standard test method for microscopical determination of parameters of the air-void system in hardened concrete*. ASTM International.

Guo, S., Dai, Q., Sun, X., & Sun, Y. (2016, June). Ultrasonic scattering measurement of air void size distribution in hardened concrete samples. *Construction and Building Materials*, *113*, 415–422. https://doi.org/10.1016/j.conbuildmat.2016.03.051

Guo, S., Dai, Q., Sun, X., Sun, Y., & Liu, Z. (2017, March). Ultrasonic techniques for air void size distribution and property evaluation in both early-age and hardened concrete samples. *Applied Sciences*, *7*(3), 290. https://doi.org/10.3390/app7030290

Jakobsen, U. H., Pade, C., Thaulow, N., Brown, D., Sahu, S., Magnusson, O., De Buck, S., & De Schutter, G. (2006). Automated air void analysis of hardened concrete—a round robin study. *Cement and Concrete Research*, *36*(8), 1444–1452.

Jana, D. (2007). A round robin test on measurements of air void parameters in hardened concrete by various automated image analyses and ASTM C 457 methods. *Proceedings of the 29th International Conference on Cement Microscopy* (pp. 26–28).

Ley, M. T. (2007). *The effects of fly ash on the ability to entrain and stabilize air in concrete* [Doctoral dissertation, The University of Texas at Austin]. http://hdl.handle.net/2152/3331

Mehta, P. K., & Monteiro, P. J. M. (2014). *Concrete: microstructure, properties, and materials*. McGraw-Hill Education.

Peterson, K., Sutter, L., & Radlinski, M. (2009, October). The practical application of a flatbed scanner for air-void characterization of hardened concrete. *Journal of ASTM International*, *6*(9), 1–15.

Punurai, W., Jarzynski, J., Qu, J., Kim, J.-Y., Jacobs, L. J., & Kurtis, K. E. (2007, January). Characterization of multi-scale porosity in cement paste by advanced ultrasonic techniques. *Cement and Concrete Research*, *37*(1), 38–46. https://doi.org/10.1016/j.cemconres.2006.09.016

Punurai, W., Jarzynski, J., Qu, J., Kurtis, K. E., & Jacobs, L. J. (2006, September). Characterization of entrained air voids in cement paste with scattered ultrasound. *NDT & E International*, *39*(6), 514–524. https://doi.org/10.1016/j.ndteint.2006.02.001

Saucier, F., Pleau, R., & Vézina, D. (1996, October). Precision of the air void characteristics measurement by ASTM C 457: results of an interlaboratory test program. *Canadian Journal of Civil Engineering*, *23*(5), 1118–1128. https://doi.org/10.1139/l96-919

Shang, H.-S., & Yi, T.-H. (2013). Freeze-thaw durability of air-entrained concrete. *The Scientific World Journal*, *Vol. 2013*, pp. 1–6. https://doi.org/10.1155/2013/650791

Simon, M. J. (2005, December). *An interlab evaluation of the variability in the ASTM C 457 linear traverse method* (Final Report RI98-006B). Missouri Department of Transportation.

Song, Y., Zou, R., Castaneda, D. I., Riding, K. A., & Lange, D. A. (2017). Advances in measuring air-void parameters in hardened concrete using a flatbed scanner. *Journal of Testing and Evaluation*, *45*(5), 1713–1725.

Ying, C. F., & Truell, R. (1956, September 1). Scattering of a plane longitudinal wave by a spherical obstacle in an isotropically elastic solid. *Journal of Applied Physics*, *27*(9), 1086–1097. https://doi.org/10.1063/1.1722545

Zhang, C., Wang, X., Yan, Q., Vipulanandan, C., & Song, G. (2020, July). A novel method to monitor soft soil strength development in artificial ground freezing projects based on electromechanical impedance technique: Theoretical modeling and experimental validation. *Journal of Intelligent Material Systems and Structures*, *31*(12), 1477–1494. https://doi.org/10.1177/1045389X20919973

About the Joint Transportation Research Program (JTRP)

On March 11, 1937, the Indiana Legislature passed an act which authorized the Indiana State Highway Commission to cooperate with and assist Purdue University in developing the best methods of improving and maintaining the highways of the state and the respective counties thereof. That collaborative effort was called the Joint Highway Research Project (JHRP). In 1997 the collaborative venture was renamed as the Joint Transportation Research Program (JTRP) to reflect the state and national efforts to integrate the management and operation of various transportation modes.

The first studies of JHRP were concerned with Test Road No. 1—evaluation of the weathering characteristics of stabilized materials. After World War II, the JHRP program grew substantially and was regularly producing technical reports. Over 1,600 technical reports are now available, published as part of the JHRP and subsequently JTRP collaborative venture between Purdue University and what is now the Indiana Department of Transportation.

Free online access to all reports is provided through a unique collaboration between JTRP and Purdue Libraries. These are available at http://docs.lib.purdue.edu/jtrp.

Further information about JTRP and its current research program is available at http://www.purdue.edu/jtrp.

About This Report

An open access version of this publication is available online. See the URL in the citation below.

Kong, Z., Mitra, A. R., & Lu, L. (2024). *Developing AI-assisted in-situ NDT method for air-void distribution testing in fresh and hardened concrete* (Joint Transportation Research Program Publication No. FHWA/IN/JTRP-2024/12). West Lafayette, IN: Purdue University. https://doi.org/10.5703/1288284317745